Nonlinear Distortion Noise and Linear Attenuation in MIMO Systems—Theory and Application to Multiband Transmitters

Daniel Rönnow and Peter Händel, *Senior Member, IEEE*

***Abstract*—Nonlinear static multiple-input multiple-output (MIMO) systems are analyzed. The matrix formulation of Bussgang's theorem for complex Gaussian signals is rederived and put in the context of the multivariate cumulant series expansion. The attenuation matrix is a function of the input signals' covariance and the covariance of the input and output signals. The covariance of the distortion noise is in addition a function of the output signal's covariance. The effect of the observation bandwidth is discussed. Models of concurrent multiband transmitters are analyzed. For a transmitter with dual non-contiguous bands expressions for the normalized mean square error (NMSE) vs input signal power are derived for uncorrelated, partially correlated, and correlated input signals. A transmitter with arbitrary number of non-contiguous bands is analysed for correlated and uncorrelated signals. In an example, the NMSE is higher when the input signals are correlated than when they are uncorrelated for the same input signal power and it increases with the number of frequency bands. A concurrent dual band amplifier with contiguous bands is analyzed; in this case the NMSE depends on the bandwidth of the aggregated signal.**

***Index Terms*—Bussgang theory, carrier aggregation, concurrent dual band, MIMO, multiband transmitter, nonlinear distortion.**

I. Introduction

A STATIC nonlinear single-input single-output (SISO) system with a Gaussian input signal can be modeled as a linear system with a noise term, where the noise is uncorrelated to the input signal according to the Bussgang theorem [1]. The theorem has been used for weakly nonlinear devices [2], as well as for devices with strongly nonlinear properties such as clipping [3]. In system identification Bussgang's theorem has been used for systems with a static nonlinearity cascaded with linear filters [4], [5]. It has been extended to complex-valued signals [6] and has therefore found applications in wireless communications, in particular for signals that are similar to Gaussian signals, like orthogonal frequency domain multiplexing (OFDM) [7], [8], wideband code division multiple access [9], and filter bank-based multicarrier [7] signals. In telecommunication Bussgang's theorem has been used in the derivation of decoding algorithms in receivers for decoding of nonlinearly distorted signals [10] and for analyzing the effect on bit error rate from nonlinear amplifiers [7].

The Bussgang theorem can be derived as a special case of the cumulant expansion of the covariance of the output and input signals, when the static nonlinear system is described by an analytic function. The cumulant expansion is a Taylor series in cumulants of different order [11], [12]. For real valued Gaussian [11] and circular complex Gaussian variables [12] only cumulants of order up to two are non-zero. For zero mean signals the first order cumulants become zero and the Bussgang theorem is obtained, since the second order cumulant is the variance.

Nonlinear multiple-input multiple-output (MIMO) systems and devices have attracted interest because of the applications in wireless communications. Bussgang's theorem can be used for MIMO transmitters, in which case the system is decomposed such that a part is a nonlinear static SISO system to which the theorem can be applied [13], [14]. In [13] an analytical expression for the optimum back-off of a 2×2 transmitter were derived using Bussgang's theorem. In [15] a frequency domain method to identify weakly nonlinear 2×2 systems is presented, where the input signals are multi-sine signals. In [16] a matrix formulation of Bussgang's theorem is derived and used to analyze the effect of quantization on MIMO channels. The matrix formalism has been used to analyze 1-bit quantization effects in transmitters [17]–[19] and receivers [20], [21] in MIMO systems, or amplifier nonlinearities [22] in MIMO systems, and quantization effects on positioning in satellite navigation systems [23]. In these applications the different signals go through different nonlinear devices and the matrix corresponding to the Bussgang attenuation in SISO systems becomes diagonal.

In telecommunication multiband transmitters have attracted attention the last years. In such transmitters, baseband signals are upconverted to different center frequencies and amplified [24]. The output signals at different center frequencies are downconverted separately in the receivers and such transmitters are therefore analyzed as MIMO systems. Concurrent dual or multiband transmitters are used in telecommunication [25] and wireless sensor networks [26], [27] applications. In these transmitters multiple signals go through the same nonlinear device.

Manuscript received November 16, 2018; revised April 28, 2019 and June 29, 2019; accepted August 8, 2019. Date of publication August 19, 2019; date of current version September 12, 2019. The associate editor coordinating the review of this manuscript and approving it for publication was Prof. Remy Boyer. The work of D. Rönnow was supported in part by the European Commission within the European Regional Development Fund and in part by the Swedish Agency for Economic and Regional Growth, and Region Gävleborg. *(Corresponding author: Daniel Rönnow.)*

D. Rönnow is with the Department of Electronics, Mathematics and Natural Sciences, University of Gävle, 801 76 Gävle, Sweden (e-mail: daniel.ronnow@hig.se).

P. Händel is with the Department of Information Science and Engineering, KTH Royal Institute of Technology, 114 28 Stockholm, Sweden (e-mail: ph@kth.se).

Digital Object Identifier 10.1109/TSP.2019.2935896

In this paper, we rederive the matrix formalism for complex valued signals and systems in [16] and put it in the context of the multivariate cumulant expansion of a multivariate Gaussian process distorted by a nonlinear function [28]. The matrix formalism is used for systems with signals at different center frequency and the effects of observation bandwidth of the output signals and its relation to the nonlinear order are discussed. We analyze the linear attenuation and distortion noise of multiband transmitters, in which the signals go through the same nonlinear device. A decomposition into nonlinear SISO systems as in [13], [14] is not possible for such transmitters. We analyze three types of multiband transmitters. The first is a concurrent non-contiguous dual band transmitter. The effect of the correlation of the input signals is addressed. Secondly, we analyze a concurrent non-contiguous multiband transmitters and thirdly a concurrent contiguous dual band transmitter in which the two output signals at different center frequency are adjacent. The formalism could be used also for nonlinear effects in receivers, although nonlinear distortion typically is more important in transmitters.

We formulate the theory for complex-valued continuous time signals and systems; the results in Section II are valid also for real valued signals, whereas the example in Section III is for complex valued signals. Sampled signals are briefly discussed in Section II-D.

Notation: Vectors and matrices are represented by lower and upper case bold fonts ($\mathbf{u}$ and $\mathbf{U}$, respectively). $\mathbf{F}(\cdot)$ is a nonlinear static multidimensional function and $\mathbf{f}(\cdot)$ its nonlinear part. $\overline{\mathbf{U}}$, $\overline{\overline{\mathbf{U}}}$, and $\delta\mathbf{A}$ are matrices specific to a formulation of the nonlinear MIMO system. Elements of vectors and matrices are represented by italics with indices as subscript (u_i and U_{ij}, respectively). Capitals in italics, like N, are used for numbers e.g. of signals or sub-carriers. $\mathbb{E}[\cdot]$, $(\cdot)^H$, $(\cdot)^*$, and $(\cdot)^{-1}$ represent the expectation value, hermitian transpose, complex conjugate, and inverse, respectively. An index $(\cdot)_Q$ of a matrix means that the system has been rewritten to be full rank. σ_i^2 represents the variance of signal i; ρ is used for the polynomial coefficients of third order nonlinearities.

II. Theory

A. General Nonlinear MIMO Systems

We consider a time invariant static nonlinear $N \times M$ MIMO system,

$$\mathbf{r} = \mathbf{F}(\mathbf{u}), \tag{1}$$

where $\mathbf{u} \in \mathbb{C}^{N\times 1}$ are the N input signals, $\mathbf{r} \in \mathbb{C}^{M\times 1}$ the M output signals, and $\mathbf{F}(\cdot)$ is a nonlinear static function. The input signals gathered in $\mathbf{u}$ are circular complex zero mean Gaussian (ch. 2 in [29]) and may be correlated, uncorrelated or partly correlated; $\mathbf{F}(\cdot)$ is holomorphic (i.e., complex analytical or complex differentiable) [30]. In the case of non zero mean input signals, the signals can be substituted by zero mean signals, $\mathbf{u} - \mathbb{E}[\mathbf{u}]$, as in the SISO case [11].

We want to write the output signal as a linear static MIMO system

$$\mathbf{r} = \mathbf{r}_0 + \mathbf{A}\,\mathbf{u} + \mathbf{v}, \tag{2}$$

where the Bussgang attenuation $\mathbf{A} \in \mathbb{C}^{M\times N}$ is a deterministic $M \times N$ matrix, $\mathbf{v}$ is the distortion noise, and $\mathbf{r}_0 = \mathbb{E}[\mathbf{r}]$. We require that the distortion noise is uncorrelated to the input $\mathbf{u}$. We formulate the condition that the distortion noise of each channel should be uncorrelated to each input signal, i.e., the covariance matrix should be the $M \times N$ null matrix,

$$\mathbb{E}[\mathbf{v}\,\mathbf{u}^H] = \mathbf{0}. \tag{3}$$

Accordingly, using (2) and (3)

$$\mathbf{W} \triangleq \mathbb{E}[\mathbf{r}\,\mathbf{u}^H] = \mathbf{A}\,\mathbb{E}[\mathbf{u}\,\mathbf{u}^H] + \mathbb{E}[\mathbf{v}\,\mathbf{u}^H] = \mathbf{A}\,\mathbf{U}, \tag{4}$$

where $\mathbf{U} = \mathbb{E}[\mathbf{u}\,\mathbf{u}^H]$ is the covariance matrix of the input signals. From (4), we get the expression for the attenuation matrix,

$$\mathbf{A} = \mathbf{W}\mathbf{U}^{-1}, \tag{5}$$

assuming that the matrix inverse exists. We notice that the attenuation matrix in (5) is the linear minimum mean squared error estimate (cf. ch. 5 in [29]). Solving for $\mathbf{v}$ in (2) and using (3) we get the covariance of the distortion noise,

$$\mathbf{V} \triangleq \mathbb{E}[\mathbf{v}\,\mathbf{v}^H] = \mathbf{R} - \mathbf{A}\,\mathbf{U}\,\mathbf{A}^H, \tag{6}$$

where $\mathbf{R} = \mathbb{E}[(\mathbf{r} - \mathbf{r}_0)\,(\mathbf{r} - \mathbf{r}_0)^H]$.

For $N = M = 1$, (5) becomes the Bussgang attenuation and (6) the distortion noise covariance for SISO systems.

In (4) each element W_{ij} of $\mathbf{W}$ is the covariance of $F_i(u_1, \ldots, u_N)$ and u_j. Such a covariance can in general be written as a cumulant expansion [12], [28]

$$\mathbb{E}[F_i(u_1, \ldots, u_N)u_j^*] = \mathbb{E}[F_i(u_1, \ldots, u_N)]\mathbb{E}[u_j^*] + \sum_{c=1}^{N} A_{ic}\mathbb{E}[u_c u_j^*] + \mathcal{O}(3), \tag{7}$$

if $F_i(\cdot)$ is holomorphic. In (7), $\mathcal{O}(3)$ are cumulants of order three and higher and the coefficients A_{ic} are functions of the partial derivatives of $F_i(\cdot)$. If $(u_1, \ldots, u_N)$ are circular jointly Gaussian complex signals with zero mean all $\mathbb{E}[u_j^*]$ and $\mathcal{O}(3)$ terms are zero [31], which means that (4) holds and (2) can be used for a system (1). For non-Gaussian signals the $\mathcal{O}(3)$ terms are non-zero and the Bussgang theory on matrix form cannot be used.

Thus, like SISO systems, a linearization as in (2) of a system $\mathbf{F}(\cdot)$ as in (1), can be made for static MIMO systems if $\mathbf{F}(\cdot)$ is holomorphic and the input signals, $\mathbf{u}$, are zero mean circular jointly Gaussian complex signals. For real valued functions, $\mathbf{F}(\cdot)$, and signals, $\mathbf{u}$, the derivation (1) to (6) holds for $\mathbf{F}(\cdot)$ being analytic and $\mathbf{u}$ being zero mean Gaussian. For nonanalytical functions, $\mathbf{F}(\cdot)$, such as soft limiters, Bussgang's theorem can still be applied if the static nonlinear function can be written as converging series of Hermite polynomials [32].

B. Correlated Inputs and Rank

Notice that if the input signals are correlated in such a way that $K = \text{rank}(\mathbf{U}) < N$, $\mathbf{U}^{-1}$ does not exist and (5) cannot be used. In such cases the system in (1) can be reformulated as $\mathbf{r} = \mathbf{F}(\mathbf{u}(\mathbf{z}))$ with $\mathbf{u} = \mathbf{Q}\,\mathbf{z}$, where $\mathbf{Q}$ is an $N \times K$ matrix and $\mathbf{U} = \mathbf{Q}\,\mathbf{Z}\,\mathbf{Q}^H$. Instead of (2) we get $\mathbf{r} = \mathbf{A}_Q\,\mathbf{z} + \mathbf{v}_Q$ where $\mathbf{A}_Q = \mathbf{W}_Q\,\mathbf{Z}^{-1}$, where $\mathbf{W}_Q = \mathbb{E}[\mathbf{r}\,\mathbf{z}^H]$, $\mathbf{Z} = \mathbb{E}[\mathbf{z}\,\mathbf{z}^H]$,

and $\mathbf{V}_Q = \mathbb{E}[\mathbf{v}_Q\,\mathbf{v}_Q^H]$. Notice that $\mathbf{A}_Q$ is an $M \times K$, $\mathbf{Z}$ a $K \times K$, and $\mathbf{V}_Q$ an $M \times M$ matrix.

C. Nonlinear Systems With a Linear Term

We now consider a nonlinear system with a linear term

$$\mathbf{r} = \mathbf{F}(\mathbf{u}) = \mathbf{H}\,\mathbf{u} + \mathbf{G}\,\mathbf{f}(\mathbf{u}), \tag{8}$$

where $\mathbf{H}$ and $\mathbf{G}$ are a $M \times N$ matrices, and $\mathbf{f}(\mathbf{u})$ is the nonlinear part of $\mathbf{F}(\mathbf{u})$. Using (8) in (4) gives

$$\mathbf{W} = \mathbf{H}\,\underbrace{\mathbb{E}[\mathbf{u}\,\mathbf{u}^H]}_{\mathbf{U}} + \mathbf{G}\,\underbrace{\mathbb{E}[\mathbf{f}(\mathbf{u})\,\mathbf{u}^H]}_{\overline{\mathbf{U}}} \tag{9}$$

and (5) and (9) gives

$$\mathbf{A} = [\mathbf{H}\,\mathbf{U} + \mathbf{G}\,\overline{\mathbf{U}}]\mathbf{U}^{-1} = \mathbf{H} + \underbrace{\mathbf{G}\,\overline{\mathbf{U}}\,\mathbf{U}^{-1}}_{\delta\mathbf{A}}, \tag{10}$$

i.e. for nonlinear systems with a linear term, the attenuation matrix $\mathbf{A}$ in (2) can be written as a sum of the linear part in (8), $\mathbf{H}$, and a matrix, $\delta\mathbf{A}$, which is a function of the nonlinear part, $\mathbf{f}(\mathbf{u})$, in (8) and $\mathbf{u}$. Inserting (8) in (6) gives

$$\mathbf{V} = \mathbf{G}\,(\overline{\overline{\mathbf{U}}} - \overline{\mathbf{U}}\,\mathbf{U}^{-1}\,\overline{\mathbf{U}}^H)\,\mathbf{G}^H, \tag{11}$$

where

$$\overline{\overline{\mathbf{U}}} = \mathbb{E}[\mathbf{f}(\mathbf{u})\,\mathbf{f}(\mathbf{u})^H]. \tag{12}$$

The covariance matrix $\mathbf{V}$ of the distortion error $\mathbf{v}$ is a function of the matrix $\mathbf{G}$ of the nonlinear part in (8), and the moment properties of the input signal $\mathbf{u}$ via $\mathbf{U}^{-1}$, $\overline{\mathbf{U}}$ and $\overline{\overline{\mathbf{U}}}$.

If the system in (8) is not full rank and we use $\mathbf{u} = \mathbf{Q}\mathbf{z}$, (8) becomes

$$\mathbf{r} = \mathbf{F}(\mathbf{u}(\mathbf{z})) = \mathbf{H}_Q\,\mathbf{z} + \mathbf{G}\,\mathbf{f}(\mathbf{u}(\mathbf{z})), \tag{13}$$

where $\mathbf{H}_Q = \mathbf{H}\mathbf{Q}$. Furthermore, $\mathbf{W}$, $\mathbf{H}$, $\mathbf{A}$, $\mathbf{U}$, $\overline{\mathbf{U}}$, and $\overline{\overline{\mathbf{U}}}$ are replaced by $\mathbf{W}_Q$, $\mathbf{H}_Q$, $\mathbf{A}_Q$, $\mathbf{Z}$, $\overline{\mathbf{Z}}$, and $\overline{\overline{\mathbf{Z}}}$, respectively, in (9)–(12).

D. Multiple Bands and Observation Bandwidth

We analyze transmitters for multiple frequency bands using continuous time complex baseband models. In Fig. 1 the cases of non-contiguous signals (top) and contiguous signals (bottom) are illustrated. The bandwidth of the input signals is B and the maximum nonlinear order is P.

In the non-contiguous case, the baseband signals, u_ℓ are upconverted to different center frequencies, that are widely separated. The nonlinear distortion at one center frequency, is affected by both input signals, if the input signals goes through the same nonlinear element. We use the observation bandwidth $P \times B$ for each output signal, which is wide enough to comprehend the distorted signal around its center frequency. The different output signals, r_ℓ, are, thus, observed independently.

In Fig. 1 (bottom) the case of two contiguous signals in one band is illustrated. The two adjacent signals form one output signal in one band. The out-of-band distortion of one signal leaks into the band of the other. The aggregated output signal, r, is observed. The observation bandwidth, $(P+1) \times B$, is wide enough to comprehend the aggregated signal.

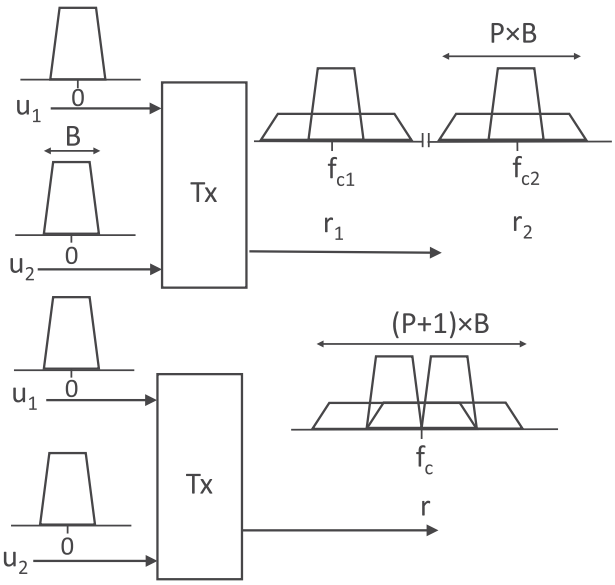

Fig. 1. Illustration of the frequency bands of the input signals, u_1 and u_2, and output signals r_1 and r_2 (top) and r (bottom) of nonlinear concurrent dual band transmitters. The top figure shows the case of non-contiguous bands with output signals, r_1 and r_2, observed at center frequencies f_{c1} and f_{c2}, respectively. The bottom figure shows the case of contiguous bands aggregated to a signal r observed at a center frequency of f_c. B is the bandwidth of the input signals and P is the maximum nonlinear order.

In complex baseband models of bandpass systems, like radio frequency amplifiers, the nonlinearites are odd functions and, hence, $\mathbf{r}_0 = \mathbf{0}$ in (2).

The nonlinear distortion gives an in-band error (within the bandwidth B) and out-of-band error (outside of B), both of which are parts of the distortion noise, $\mathbf{v}$. Combining (8) and (2) with $\mathbf{r}_0 = \mathbf{0}$, we get

$$\mathbf{v} = (\mathbf{H} - \mathbf{A})\mathbf{u} + \mathbf{G}\mathbf{f}(\mathbf{u}), \tag{14}$$

where the term $(\mathbf{H} - \mathbf{A})\mathbf{u}$ contributes to the in-band error; the term $\mathbf{G}\mathbf{f}(\mathbf{u})$ contributes to the error within the bandwidth $P \times B$ or $(P+1) \times B$, respectively, i.e., it contributes to the error both in-band and out-of-band. The in-band error is uncorrelated to the input signal and Bussgang's theorem can be used also for the in-band error [33]. However, the in-band error is a filtered version of the distortion noise caused by the static nonlinearity.

In the derivation above, as in the derivations of Bussgang's theorem for a SISO system, it is assumed that the distorted signals, $\mathbf{r}$, are caused by static nonlinearities. Thus, the observation bandwidth has to be large enough to observe the entire signal. In Fig. 1 (top) it should be $P \times B$ and in Fig. 1 (bottom) it should be $(P+1) \times B$. Smaller observation bandwidths could be relevant if the effects of non-ideal receivers are of interest. For example, an observation bandwidth equal to the undistorted signals' bandwidths can be used (B and $2 \times B$, respectively, in Fig. 1) if the signal is not filtered before observation. In such cases the out-of-band distortion is aliased in-band and the distortion error's variance is unchanged.

The sampling rate has to be considered in the case of discrete time models of the nonlinear transmitters and in the case of non ideal receivers. Ideally, the Nyquist frequency - when sampling

the down converted signal - should be $P \times B/2$ and $(P+1) \times B/2$ in the cases in Fig. 1 (top) and (bottom), respectively.

III. Application to Concurrent Dual Band Transmitter

In a concurrent non-contiguous dual band transmitter there are two or more signals at widely separated carrier frequencies, as shown in Fig. 1 (top).

In an application where the signals are for different users the signals would be uncorrelated. Concurrent non-contiguous dual or multiband transmitters used in telecommunication base stations would be such an application. Partly correlated signals could occur if such transmitters are used in dual or multi frequency wireless sensor networks [26] with network coding. Using network coding, data packages of different users can be mixed when forwarded by a wireless node [27]. Correlated signals occur as a special case in this type of application. In both telecommunication and wireless sensor network applications signals that are similar to zero mean circular complex Gaussian signals, such as OFDM, are used.

In this section a concurrent non-contiguous dual band transmitter model with nonlinear distortion is investigated using the formalism in Section II for uncorrelated, correlated, and partly correlated input signals. We give more details for the correlated case to illustrate the method. We analyze a transmitter architecture in which the two signals are fed through the same nonlinear amplifier [24].

A. Nonlinear Device Model

The largest hardware impairment in radio frequency amplifiers is typically the static third order nonlinear distortion. The third order intercept point - a common quality measure - relates the inter-modulation distortion to the polynomial parameter of third order [34]. A complex-valued baseband behavioral model [35] with normalized small signal gain including the main impairments in the form of (8) is

$$\mathbf{r} = \underbrace{\begin{pmatrix} 1 & 0 \\ 0 & 1 \end{pmatrix}}_{\mathbf{H}=\mathbf{I}} \mathbf{u} + \underbrace{\begin{pmatrix} \rho_{1,1} & 0 & \rho_{1,2} & 0 \\ 0 & \rho_{2,1} & 0 & \rho_{2,2} \end{pmatrix}}_{\mathbf{G}} \underbrace{\begin{pmatrix} u_1 |u_1|^2 \\ u_2 |u_1|^2 \\ u_1 |u_2|^2 \\ u_2 |u_2|^2 \end{pmatrix}}_{\mathbf{f}(\mathbf{u})}, \tag{15}$$

where $\{\rho_{1,1},\, \rho_{2,2}\} \in \mathbb{C}$ cause inter-modulation distortion and $\{\rho_{1,2},\, \rho_{2,1}\} \in \mathbb{C}$ cause cross-modulation distortion [36]. The input signals u_1 and u_2 are complex baseband representations of the signals at the different center frequencies. The thermal noise, $\mathbf{n}$, is in general modelled as added at the output of the amplifier, [34]

$$\mathbf{y} = \mathbf{r} + \mathbf{n}, \tag{16}$$

where the thermal noise is uncorrelated, but with the same variance, σ_n^2, in both channels, i.e., the thermal noise covariance is $\mathbf{N} = \sigma_n^2 \mathbf{I}$. Notice that σ_n^2 is the variance of the noise within the observation bandwidth.

The model in (15) cannot be decomposed into SISO subsystems that are static nonlinearities, such that the SISO Bussgang theorem can be used. In such decompositions the input signal of each SISO system is a linear combination of the input signals to the MIMO system. The reason is that the model in (15) includes baseband signals in each frequency band and that the corresponding radio frequency signals of different center frequency are fed through the same nonlinear amplifier; there are nonlinear but not any linear cross-terms.

B. Linear Device Model - Uncorrelated Signals

In the case of uncorrelated signals the input signals $\mathbf{u} = (u_1\ u_2)^T$ are complex-valued uncorrelated zero-mean Gaussian, with

$$\mathbf{U} = \begin{pmatrix} \sigma_1^2 & 0 \\ 0 & \sigma_2^2 \end{pmatrix}. \tag{17}$$

We determine the matrices $\mathbf{A}$ and $\mathbf{V}$ that describe the system in (15) on the form in (2). We first determine $\overline{\mathbf{U}}$ and $\overline{\overline{\mathbf{U}}}$. The matrix $\overline{\mathbf{U}}$ reads

$$\overline{\mathbf{U}} = \mathbb{E}\left[\begin{pmatrix} u_1 |u_1|^2 \\ u_2 |u_1|^2 \\ u_1 |u_2|^2 \\ u_2 |u_2|^2 \end{pmatrix} (u_1^*\ u_2^*) \right] = \begin{pmatrix} 2\sigma_1^4 & 0 \\ 0 & \sigma_1^2\,\sigma_2^2 \\ \sigma_1^2\,\sigma_2^2 & 0 \\ 0 & 2\sigma_2^4 \end{pmatrix}, \tag{18}$$

where it has been used that the odd order moments equal zero. Further, it was used that $\mathbb{E}[(u_\ell\, u_\ell^*)^n] = n!\, \mathbb{E}[u_\ell\, u_\ell^*]^n$ for positive integers n and $\ell = 1,\ 2$, where ! denotes the factorial operation [13].

For the matrix $\overline{\overline{\mathbf{U}}}$ we get

$$\overline{\overline{\mathbf{U}}} = \mathbb{E}\left[\begin{pmatrix} u_1 |u_1|^2 \\ u_2 |u_1|^2 \\ u_1 |u_2|^2 \\ u_2 |u_2|^2 \end{pmatrix} \left(u_1^* |u_1|^2 \ \ u_2^* |u_1|^2 \ \ u_1^* |u_2|^2 \ \ u_2^* |u_2|^2 \right) \right]$$

$$= \begin{pmatrix} 6\sigma_1^6 & 0 & 2\sigma_1^4\,\sigma_2^2 & 0 \\ 0 & 2\sigma_1^4\,\sigma_2^2 & 0 & 2\sigma_1^2\,\sigma_2^4 \\ 2\sigma_1^4\,\sigma_2^2 & 0 & 2\sigma_1^2\,\sigma_2^4 & 0 \\ 0 & 2\sigma_1^2\,\sigma_2^4 & 0 & 6\sigma_2^6 \end{pmatrix}. \tag{19}$$

In (18) and (19) the sixth order moments were calculated as described in [13].

Using (15), (17), (18), and (19) in (10) we get

$$\mathbf{A} = \begin{pmatrix} 1 + 2\rho_{1,1}\,\sigma_1^2 + \rho_{1,2}\,\sigma_2^2 & 0 \\ 0 & 1 + 2\rho_{2,2}\,\sigma_2^2 + \rho_{2,1}\,\sigma_1^2 \end{pmatrix}. \tag{20}$$

Using (15), (17), (18), and (19) in (11) we get the covariance of the distortion noise

$$\mathbf{V} = \begin{pmatrix} 2|\rho_{1,1}|^2\,\sigma_1^6 + |\rho_{1,2}|^2\,\sigma_1^2\sigma_2^4 & 0 \\ 0 & 2|\rho_{2,2}|^2\,\sigma_2^6 + |\rho_{2,1}|^2\,\sigma_1^4\sigma_2^2 \end{pmatrix}. \tag{21}$$

Notice that $\mathbf{A}$ is diagonal, i.e. r_1 is linearly proportional to u_1 but not to u_2. However, the element A_{11} contains σ_2^2, which means that r_1 depends on u_2 through its variance σ_2^2. $\mathbf{V}$ is also

diagonal, which means that the error signals of channels 1 and 2 are uncorrelated.

As a measure of the device performance we use the normalized mean square error (NMSE), which for channel ℓ is [37]

$$\text{NMSE}_\ell = \frac{\mathbb{E}[e_\ell e_\ell^*]}{\sigma_\ell^2}, \tag{22}$$

where $e_\ell = y_\ell - u_\ell$. Using (20) and (21) with (2) and (16) we get for the concurrent dual band amplifier with uncorrelated input signals

$$\text{NMSE}_\ell = 6|\rho_{\ell\ell}|^2\,\sigma_\ell^4 + 2|\rho_{\ell k}|^2\,\sigma_k^4 + 4\Re[\rho_{\ell\ell}\,\rho_{\ell k}^*]\sigma_l^2\,\sigma_k^2 + \frac{\sigma_n^2}{\sigma_\ell^2}, \tag{23}$$

where $k, \ell = 1, 2$ or $2, 1$. The three first terms are proportional to the square of the power of the input signal; the fourth term is proportional to the inverse of the signal power. The two first terms do not depend on the phase of $\rho_{\ell\ell}$ and $\rho_{\ell k}$ whereas the third term depends on $\rho_{\ell\ell}\rho_{\ell k}$. The effect on the NMSE from nonlinear distortion is large at high values of σ_ℓ^2 and σ_k^2.

C. Linear Device Model - Correlated Signals

In the case of correlated signals we model the input signals as $u_1 = u_2$ and the system's rank becomes 1 instead of 2. We use $\mathbf{Q} = (1\ 1)^T$; we set $u_1 = u_2 = z$ and the covariance of z becomes scalar $\mathbf{Z} = \sigma^2$. We derive $\mathbf{A}_Q$ and $\mathbf{V}_Q$ as described in Section II-B. For the attenuation matrix we get

$$\mathbf{A}_Q = \begin{pmatrix} 1 + 2\sigma^2(\rho_{1,1} + \rho_{1,2}) \\ 1 + 2\sigma^2(\rho_{2,2} + \rho_{2,1}) \end{pmatrix}, \tag{24}$$

for the covariance of the distortion noise we get

$$\mathbf{V}_Q = 2\sigma^6 \times \begin{pmatrix} |\rho_{1,1}+\rho_{1,2}|^2 & (\rho_{1,1}+\rho_{1,2})(\rho_{2,2}+\rho_{2,1})^* \\ (\rho_{1,1}+\rho_{1,2})^*(\rho_{2,2}+\rho_{2,1}) & |\rho_{2,2}+\rho_{2,1}|^2 \end{pmatrix}, \tag{25}$$

and for the NMSE

$$\text{NMSE}_\ell = 6|\rho_{\ell\ell} + \rho_{\ell k}|^2\,\sigma^4 + \frac{\sigma_n^2}{\sigma^2}, \tag{26}$$

where $\ell = 1$ or 2. The first term is proportional to the square of the input signal power, σ^4, and dominates the NMSE at large input signal power. Notice that in the first term the complex numbers $\rho_{\ell\ell}$ and $\rho_{\ell k}$ are added and this term could become zero.

D. Linear Device Model - Partly Correlated Signals

Partly correlated signals are modeled as $u_1 = u_c + u_{1u}$ and $u_2 = u_c + u_{2u}$ where u_c with variance σ_c^2 is the correlated part identical for both signals and u_{1u} and u_{2u} with variance σ_{1u} and σ_{2u} are the uncorrelated parts of u_1 and u_2, respectively [38]. The signals u_{1u} and u_{2u} are also uncorrelated to u_c. The covariance matrix of $\mathbf{u}$ is

$$\mathbf{U} = \begin{pmatrix} \sigma_c^2 + \sigma_{1u}^2 & \sigma_c^2 \\ \sigma_c^2 & \sigma_c^2 + \sigma_{2u}^2 \end{pmatrix}. \tag{27}$$

We follow the derivations in Section III-B, but for partly correlated signals. For the attenuation matrix, $\mathbf{A}$, we get the elements

$$\begin{aligned} A_{\ell\ell} = 1 &+ 2\rho_{\ell,\ell}[\sigma_c^4(\sigma_{\ell u}^2 + \sigma_{ku}^2) \\ &+ \sigma_c^2\sigma_{\ell u}^2(\sigma_{\ell u}^2 + 2\sigma_{ku}^2) + 2\sigma_{\ell u}^4\sigma_{ku}^2]/\gamma \\ &+ \rho_{\ell,k}[\sigma_c^4(\sigma_{\ell u}^2 + \sigma_{ku}^2) + \sigma_c^2\sigma_{ku}^2(2\sigma_{\ell u}^2 + \sigma_{ku}^2) \\ &+ \sigma_{\ell u}^2\sigma_{ku}^4]/\gamma \end{aligned} \tag{28}$$

and

$$A_{\ell k} = \rho_{\ell,k}\sigma_c^2[\sigma_c^2(\sigma_{\ell u}^2 + 2\sigma_{ku}^2) + \sigma_{\ell u}^2\sigma_{ku}^2]/\gamma, \tag{29}$$

where $\gamma = \sigma_c^2(\sigma_{\ell u}^2 + \sigma_{ku}^2) + \sigma_{\ell u}^2\sigma_{ku}^2$ and $k, \ell = 1, 2$ or $2, 1$. The distortion noise covariance, $\mathbf{V}$, becomes

$$\begin{aligned} V_{\ell\ell} = 2|\rho_\ell|^2(\sigma_c^2 + \sigma_{\ell u}^2)^3 &+ 2(\rho_\ell^*\xi_\ell + \rho_\ell\xi_\ell^*)\sigma_c^4(\sigma_c^2 + \sigma_{\ell u}^2) \\ &+ |\xi_\ell|^2(2\sigma_c^6 + \sigma_c^4(\sigma_{\ell u}^2 + 3\sigma_{ku}^2) \\ &+ \sigma_c^2(2\sigma_{\ell u}^2\sigma_{ku}^2 + \sigma_{2u}^4) + \sigma_{\ell u}^2\sigma_{ku}^4) \end{aligned} \tag{30}$$

and

$$\begin{aligned} V_{\ell k} = 2\rho_\ell\rho_k^*\sigma_c^6 &+ 2\rho_k^*\xi_\ell\sigma_c^2(\sigma_c^4 + 2\sigma_c^2\sigma_{ku}^2 + \sigma_{ku}^4) \\ &+ 2\rho_\ell\xi_k^*\sigma_c^2(\sigma_c^4 + 2\sigma_c^2\sigma_{\ell u}^2 + \sigma_{\ell u}^4) \\ &+ \xi_\ell\xi_k^*\sigma_c^2(2\sigma_c^4 + \sigma_c^2(\sigma_{\ell u}^2 + \sigma_{ku}^2) + \sigma_{\ell u}^2\sigma_{ku}^2), \end{aligned} \tag{31}$$

where $k, \ell = 1, 2$ or $2, 1$. The NMSE becomes

$$\begin{aligned} \text{NMSE}_\ell = (&|A_{\ell\ell} + A_{\ell k} - 1|^2\sigma_c^2 + |A_{\ell\ell} - 1|^2\sigma_{\ell u}^2 \\ &+ |A_{\ell k}|^2\sigma_{ku}^2 + V_{\ell\ell} + \sigma_n^2)/(\sigma_c^2 + \sigma_{lu}^2), \end{aligned} \tag{32}$$

where $k, \ell = 1, 2$ or $2, 1$ and $A_{\ell\ell}$ and $A_{\ell k}$ are given by (28) and $V_{\ell\ell}$ by (30).

For $\sigma_c^2 = 0$, $\mathbf{A}$ in (28) becomes identical to the uncorrelated case (20), and $\mathbf{V}$ in (30) becomes identical to (21) as expected.

For $\sigma_{1u}^2 = \sigma_{2u}^2 = 0$, we get from (28) and (24) that $A_{Q,\ell\ell} = A_{\ell\ell} + A_{\ell k}$; furthermore comparing (30) and (25) we see that $\mathbf{V} = \mathbf{V}_Q$.

E. Device Performance

We now illustrate how the Bussgang attenuation matrix, the distortion noise covariance, and then NMSE - as derived in Sections III-B to III-D - vary with signal power and correlation. For comparison, we simulate the device in Section III-A numerically and compare the results with the analytical results in Sections III-B to III-D. We denote the simulated output signal $\mathbf{y}_{sim}$. We use $\rho_{1,1} = 0.38\angle -90^\circ$ and $\rho_{1,2} = 0.38\angle 0^\circ$ (where $\angle$ denotes the phase angle) that we estimate from measurements of third order inter- and cross-modulation products described in [36]; the signal powers are in relative units.

We made four sets of simulations:

1) Uncorrelated signals with $\sigma_1^2 = \sigma_2^2$ and σ_1^2 was varied from -12 dB to 3 dB.
2) Uncorrelated signals with σ_1^2 varied from -12 dB to 3 dB, while σ_2^2 was fixed at first -0 dB and then -9 dB.
3) Correlated signals with $\sigma_1^2 = \sigma_2^2 = \sigma^2$ varied from -12 dB to 3 dB.
4) Partly correlated signals with the correlation ratio, $\sigma_c^2/(\sigma_c^2 + \sigma_{2u}^2)$ varied from 0 to 1, while $\sigma_1^2 = \sigma_c^2 + \sigma_{1u}^2$ and $\sigma_2^2 = \sigma_c^2 + \sigma_{2u}^2$ were fixed at 0 dB.

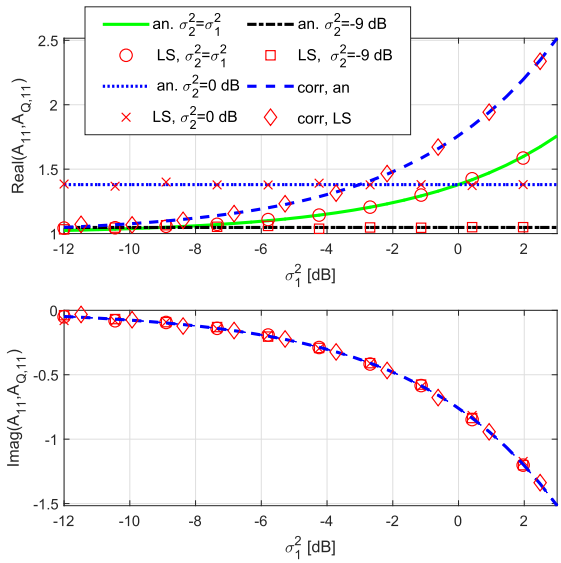

Fig. 2. Real and imaginary parts of elements of the attenuation matrices (A_{11} and $A_{Q,11}$) vs input power, σ_1^2, as calculated analytically (an) and from the simulated data (LS) for a concurrent non-contiguous dual band transmitter. Data for uncorrelated and correlated input signals are shown. For the imaginary part (lower figure) the lines are on top of each other.

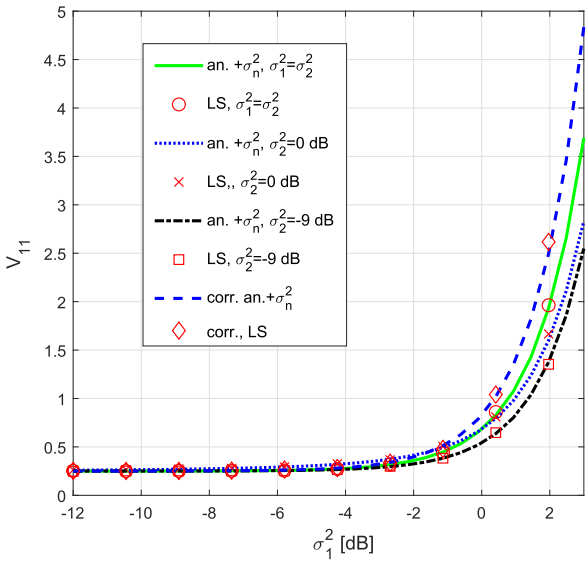

Fig. 3. The noise variance of channel 1 vs input power, σ_1^2, as calculated analytically (an), and from the simulated data (LS) for a concurrent non-contiguous dual band transmitter. For the analytical data $V_{11}+\sigma_n^2$ is shown. Data for uncorrelated and correlated input signals are shown.

In all simulations the thermal noise power was $\sigma_n^2 = -6$ dB and the signals had a length of 10000 samples.

The attenuation $\mathbf{A}$ was determined in the least square (LS) sense, $\mathbf{A}_{LS} = \mathbf{y}_{sim}\mathbf{u}^H(\mathbf{u}\mathbf{u}^H)^{-1}$ [39]. The noise covariance, $\mathbf{V}_{LS}$ was determined as the covariance of $\mathbf{e} = \mathbf{y}_{sim} - \mathbf{y}_{LS}$, where $\mathbf{y}_{LS} = \mathbf{A}_{LS}\mathbf{u}$.

In Fig. 2 the element A_{11} from the simulations 1, 2, and 3 is shown vs input power, σ_1^2 (LS); A_{11} as obtained analytically from (20) and from (24), respectively, is also shown. The LS and analytical data are as expected in agreement.

For uncorrelated signals and $\sigma_1^2 = \sigma_2^2$ both the real and imaginary parts of A_{11} change with σ_1^2. For uncorrelated signals and σ_2^2 constant and σ_1^2 varied, the real part of A_{11} is constant and the imaginary part changes with σ_1^2, because $\rho_{1,1}$ is imaginary but $\rho_{1,2}$ is real in (20). Notice that the attenuation matrix can have complex elements, A_{11} though the small signal gain (the element H_{11}) is real valued. The LS estimates of A_{12} and A_{21} (not shown in the figure) were close to zero in agreement with (20).

The real part of $A_{Q,11}$ increases faster with the input power than the real part of A_{11}, but the imaginary part is identical, since $\rho_{1,1}$ is imaginary and $\rho_{1,2}$ is real.

The LS estimates, $\mathbf{A}_{LS}$, are unbiased since the noise terms in (2) have zero mean in this case [40], as seen in Fig. 2.

Fig. 3 shows the simulated noise variance of channel 1 vs σ_1^2 for the simulations 1, 2, and 3 (LS). Also shown is V_{11} as determined from (21) and (25), respectively. We plot the analytical $V_{11}+\sigma_n^2$, since it corresponds to the covariance of the simulated data. The LS data are as expected in agreement with the analytical $V_{11}+\sigma_n^2$. As expected, at small values of σ_1^2, the variance is dominated by the thermal noise and at high values by the distortion noise, V_{11}. Notice that V_{11} also depends on the variance of u_2, σ_2^2, as seen in (21). The LS estimates

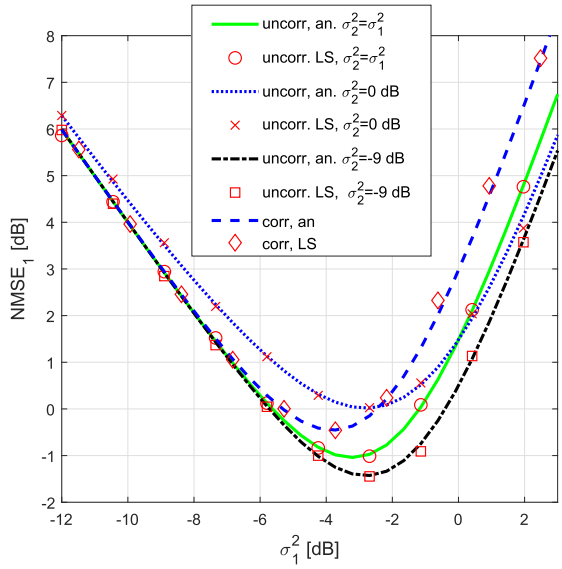

Fig. 4. NMSE of channel 1 vs input power, σ_1^2, as calculated analytically (an) and from the simulated data (LS) for a concurrent non-contiguous dual band transmitter. Data for uncorrelated and correlated input signals are shown.

of the off-diagonal elements, V_{12} and V_{21} (not shown in the figure) were close to zero in agreement with (21). In the case of correlated signals, the noise covariance is higher than in the case of uncorrelated signals and $\sigma_1^2 = \sigma_2^2$.

In Fig. 4 NMSE$_1$ vs σ_1^2 is shown for the cases of uncorrelated and correlated input signals. The analytical data are as expected in agreement with the LS data from simulations 1, 2, and 3. At low σ_1^2 values the NMSE is dominated by the thermal noise; at high values the nonlinear distortion is dominating. The effect of cross-modulation distortion is seen in the middle range of σ_1^2, where it causes the difference between the curves for $\sigma_2^2 = 0$ dB and $\sigma_2^2 = -9$ dB. For uncorrelated signals, the cross-modulation

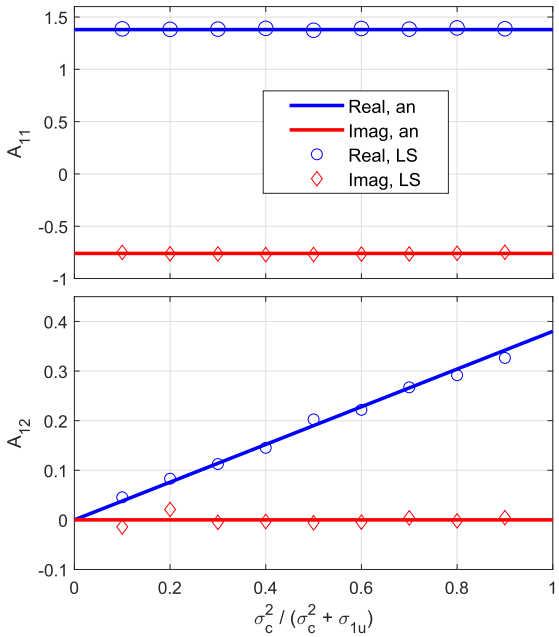

Fig. 5. The attenuation matrix elements A_{11} and A_{12} vs the correlation ratio, $\sigma_c^2/(\sigma_c^2+\sigma_{1u}^2)$, for channel 1 as obtained from analytical expressions (an) and from simulations (LS) for a concurrent non-contiguous dual band transmitter. The input powers were $\sigma_1^2=\sigma_1^2=0$ dB.

affects the NMSE vs input power in a similar way as linear cross talk in MIMO transmitters, in which two amplifiers operate at the same center frequency [13]. For high values of σ_1^2 the NMSE is higher for correlated signals than for uncorrelated signals with $\sigma_1^2=\sigma_2^2$. Thus, correlated signals give higher NMSE than uncorrelated signals for the same input power. Notice that the minimum NMSE is different for uncorrelated signals with $\sigma_1^2=\sigma_2^2$ and correlated signals. The input back-off - i.e. the input power that gives the lowest NMSE - is, thus, dependent on the correlation between the two input signals.

The results of simulations 4 are shown in Figs. 5–7. The elements A_{11} and A_{12} are shown vs correlation ratio, $\sigma_c^2/(\sigma_c^2+\sigma_{1u}^2)$, for input powers of $\sigma_1^2=0$ dB and $\sigma_2^2=0$ dB. The analytical data are obtained from (28). A_{11} and the imaginary part of A_{12} do not change with correlation ratio, whereas the real part of A_{12} changes linearly with correlation ratio.

Fig. 6 shows the distortion noise vs correlation ratio. For the analytical values of V_{11}, calculated using (30), we have added σ_n^2 to make it comparable to the simulated data. The analytical and simulated data are in agreement as expected. V_{11} increases slightly with correlation ratio and V_{12} increases from 0 to 0.6.

The NMSE of channel 1 increases monotonically by 1.5 dB with correlation ratio as seen in Fig. 7. The analytical data, obtained using (32), and simulated data (LS) are in agreement.

We have assumed Gaussian signals in the derivations of $\mathbf{A}$ and $\mathbf{V}$. In [41] expressions for $\delta A_{\ell\ell}$ and $V_{\ell\ell}$ are derived for SISO third order nonlinearities for OFDM signals that are not ideally Gaussian because the number of subcarriers, N_s, is finite. Their expressions can be applied to our case

$$\delta\mathbf{A}_{OFDM}=\delta\mathbf{A}\left(1-\frac{1}{2N_s}\right), \tag{33}$$

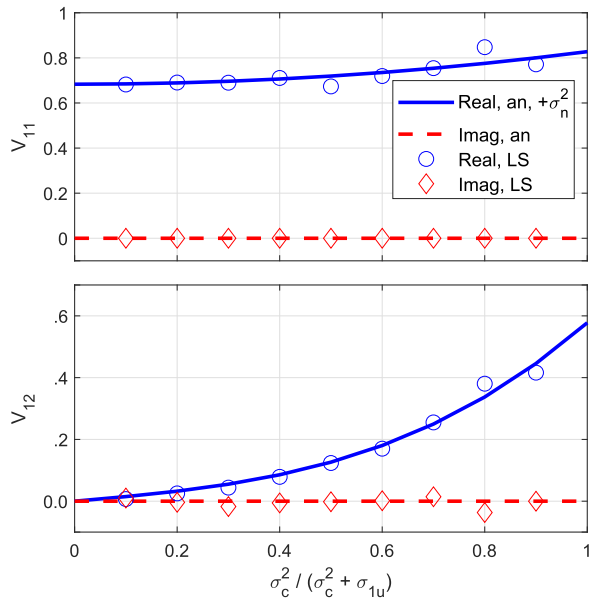

Fig. 6. The distortion noise covariance V_{11} and V_{12} vs the correlation ratio, $\sigma_c^2/(\sigma_c^2+\sigma_{1u}^2)$, for channel 1 as obtained from analytical expressions (an) and from simulations (LS) for a concurrent non-contiguous dual band amplifier. The input powers were $\sigma_1^2=\sigma_1^2=0$ dB.

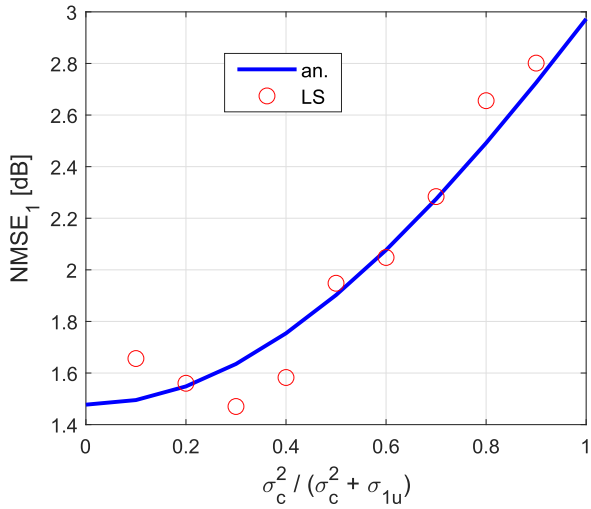

Fig. 7. NMSE of channel 1 vs the correlation ratio, $\sigma_c^2/(\sigma_c^2+\sigma_{1u}^2)$, as obtained from analytical expressions (an) and from simulations (LS) for a concurrent non-contiguos dual band transmitter. The input powers were $\sigma_1^2=\sigma_1^2=0$ dB.

and

$$\mathbf{V}_{OFDM}=\mathbf{V}\left(1-\frac{2}{N_s}+\frac{1}{N_s^2}\right). \tag{34}$$

Typically, N_s is of the order of 10^2 to 10^3 [42]. For $N_s=10^2$ the relative errors in the elements of $\mathbf{A}$ and $\mathbf{V}$ caused by the Gaussian approximation become 0.005 (for $\Delta A_{ij}/A_{ij}$) and 0.02 (for $\Delta V_{ij}/V_{ij}$). For $N_s=10^3$ they become 0.0005 and 0.002, respectively. As a comparison the relative error in the amplitude of the coefficients for the third order nonlinearity, $\Delta\rho/\rho$, is approximately 0.5 dB or 0.05 [36]. An error analysis of $\mathbf{A}$ gives

that the relative errors, $\Delta A_{ij}/A_{ij}$, become $\delta A_{\ell,k}(\Delta\rho/\rho)$. The relative errors $\Delta V_{ij}/V_{ij}$ become $\Delta\rho/\rho$.

Thus, typically the experimental errors in the coefficients ρ gives larger errors in the elements of $\mathbf{A}$ and $\mathbf{V}$ than the Gaussian approximation.

IV. Application to Concurrent Multiple Band Transmitter

We now extend the analysis above to concurrent multiple band amplifiers with N non-contiguous bands. It corresponds to Fig. 1 (top) extended to the case with center frequencies f_{c1}, f_{c2}, ..., f_{cN}.

We analyze the cases of uncorrelated and correlated input signals. The case of partially correlated signals gives large expressions with the uncorrelated and correlated cases as special cases.

A. Nonlinear Device Model

The output signal of channel ℓ of the multiband transmitter is given by the static nonlinear function, which is an extension of (15),

$$r_\ell = u_\ell + \rho_{\ell,1}u_\ell|u_1|^2 + \rho_{\ell,2}u_\ell|u_2|^2 + \cdots + \rho_{\ell,N}u_\ell|u_N|^2, \tag{35}$$

for $\ell = 1, 2, \ldots, N$ and the output signals with added thermal noise are then given by (16). In (35) the signal in each band is distorted by third order cross-modulation terms from all other bands.

To write (35) on the same form as (15) let $\mathbf{H}$ be an $N \times N$ identity matrix and $\mathbf{G} = (\mathbf{G}_1\ \mathbf{G}_2\ \ldots\ \mathbf{G}_N)$, where $\mathbf{G}_\ell$ is a diagonal matrix with the diagonal being $(\rho_{1,\ell}\ \rho_{2,\ell}\ \ldots\ \rho_{N,\ell})$. Furthermore, $\mathbf{f}(\mathbf{u}) = (\mathbf{f}_1(\mathbf{u})\ \mathbf{f}_2(\mathbf{u})\ \ldots \mathbf{f}_N(\mathbf{u}))^T$, where $\mathbf{f}_\ell(\mathbf{u}) = (u_1|u_\ell|^2\ u_2|u_\ell|^2\ \ldots u_N|u_\ell|^2)$.

B. Linear Device Model

Following the derivations in Sections III-B and III-C, we derive $\mathbf{A}$, $\mathbf{V}$, $\mathbf{A}_Q$, $\mathbf{V}_Q$, and the corresponding NMSE for multiband amplifiers. For uncorrelated signals, $\mathbf{A}$ becomes an $N \times N$ diagonal matrix with the elements

$$A_{\ell,\ell} = 1 + 2\rho_{\ell,\ell}\sigma_\ell^2 + \sum_{k\neq\ell}\rho_{\ell,k}\sigma_k^2. \tag{36}$$

The covariance of the distortion, $\mathbf{V}$, becomes an $N \times N$ diagonal matrix with the elements

$$V_{\ell,\ell} = 2|\rho_{\ell,\ell}|^2\sigma_\ell^6 + \sum_{k\neq\ell}|\rho_{\ell,k}|^2\sigma_\ell^2\sigma_k^4 \tag{37}$$

and the NMSE for channel ℓ becomes

$$\text{NMSE}_\ell = |A_{\ell,\ell} - 1|^2 + \frac{V_{\ell,\ell}}{\sigma_\ell^2} + \frac{\sigma_n}{\sigma_\ell^2}. \tag{38}$$

For correlated signals we use $\mathbf{Q} = [1\ 1\ \ldots\ 1]^T$ and $\mathbf{A}_Q$ becomes an $N \times 1$ matrix with elements

$$A_{Q,\ell} = 1 + 2\sigma^2\sum_{k=1}^{N}\rho_{\ell,k}. \tag{39}$$

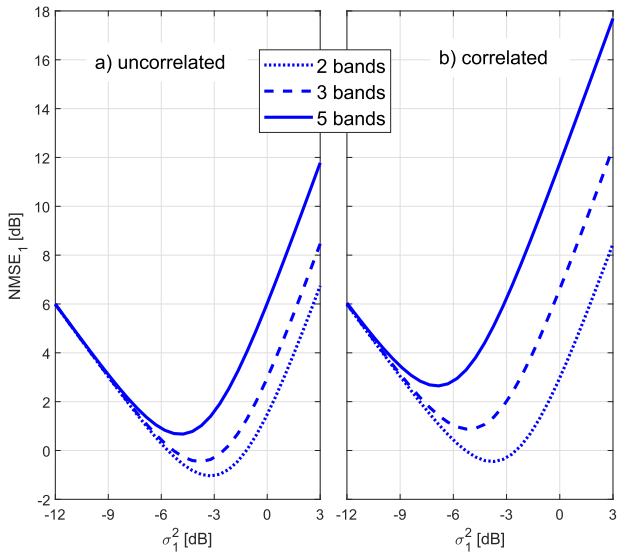

Fig. 8. NMSE of channel 1 vs the power of input signal 1 for multiband transmitters with 2, 3, and 5 bands for a) uncorrelated input signals, and b) correlated input signals.

The distortion noise covariance becomes an $N \times N$ matrix, $\mathbf{V}_Q$, with the elements

$$V_{Q,k,\ell} = 2\sigma^2\left(\sum_{m=1}^{N}\rho_{k,m}\right)\left(\sum_{m=1}^{N}\rho_{\ell,m}\right)^* \tag{40}$$

and the NMSE for channel ℓ becomes

$$\text{NMSE}_\ell = 6\sigma^4\left|\sum_{k=1}^{N}\rho_{\ell,k}\right|^2 + \frac{\sigma_n^2}{\sigma^2}. \tag{41}$$

To illustrate the device performance we set the inter-modulation and cross-modulation parameters as in the case of a concurrent dual band amplifier. For uncorrelated signals we use the same σ_ℓ^2 for all channels. We calculate the NMSE for 2, 3, and 5 bands for the cases of uncorrelated and correlated input signals using (38) and (41), respectively. In Fig. 8 the NMSE for multiband transmitters for 2, 3, and 5 bands from are shown vs input power. For all curves in Fig. 8 the NMSE is dominated by the thermal noise at low input power and by the nonlinear distortion at high input power. For both uncorrelated and correlated signals the NMSE increases with the number of bands. The NMSE is also higher for correlated than for uncorrelated input signals for these inter- and cross-modulation parameters, $\rho_{k,\ell}$. The optimum input back-off, which is the input power that gives the lowest NMSE, decreases with the number of bands for both correlated and uncorrelated signals.

V. Application to Contiguous Dual Band Transmitter

We analyze a concurrent dual band transmitter with contiguous bands, as in Fig. 1 (bottom). We analyze the case of uncorrelated input signals, which corresponds to the case of carrier aggregation [24].

A. Nonlinear Device Model

The output signal, $\mathbf{r}$, is now the aggregation of two signals shifted $\pm B/2$ relative the center frequency, f_c (cf. Fig. 1), which means that

$$\mathbf{H} = \begin{pmatrix} \mathrm{e}^{-j(B/2)t} & \mathrm{e}^{+j(B/2)t} \end{pmatrix}. \tag{42}$$

The time dependence in (42) arises from the shift in center frequency of $\mathbf{r}$ relative u_1 and u_2. For sampled output signals t becomes $(t_0, t_0 + \Delta t, \ldots)$, where t_0 is the start time and Δt is the sampling time.

For the nonlinear part, $\mathbf{f}(\mathbf{u})$ becomes the same as in (15). We assume that ρ is the same for the inter- and cross modulation of u_1 and u_2, which is justified by the fact that they are close in frequency, which gives

$$\mathbf{G} = \rho \begin{pmatrix} \mathrm{e}^{-j(B/2)t} & \mathrm{e}^{+j(B/2)t} & \mathrm{e}^{-j(B/2)t} & \mathrm{e}^{+j(B/2)t} \end{pmatrix}. \tag{43}$$

In this case the noise variance, σ_n^2, refers to the thermal noise within the observation bandwidth $(P+1) \times B$ with $P = 3$.

B. Linear Device Model

We use (42) and (43) in (10) with (17) and (18) with $\sigma_1^2 = \sigma_2^2 = \sigma^2$ and get

$$\mathbf{A} = \left(1 + 3\rho\sigma^2\right) \begin{pmatrix} \mathrm{e}^{-j(B/2)t} & \mathrm{e}^{+j(B/2)t} \end{pmatrix}. \tag{44}$$

In addition we use (19) in (11) to get

$$\mathbf{V} = 6|\rho|^2\sigma^6. \tag{45}$$

To calculate the NMSE, (22), we define the error signal of the aggregated signal as $e = y - \mathbf{H}\mathbf{u}$ and normalize by the variance of the aggregated signal, $2\sigma^2$. Using (42), (2) with $\mathbf{r}_0 = \mathbf{0}$, (16), (44) and (45) gives

$$\mathrm{NMSE} = 12|\rho|^2\sigma^4 + \frac{\sigma_n^2}{2\sigma^2}. \tag{46}$$

We compare (44)–(46) with the corresponding results for the case of non-contiguous bands in Section III-B. If we use $\rho_{\ell\ell} = \rho_{\ell k} = \rho$ and $\sigma_1^2 = \sigma_2^2 = \sigma^2$ in (20) the diagonal elements of $\mathbf{A}$ become the same as the elements of $\mathbf{A}$ in (44), except for the time dependence in the latter. The diagonal elements of $\mathbf{V}$ in (21) become the same as the elements of $\mathbf{V}$ in (45). Similarly, the NMSE in (23) becomes the same as that in (46) except for the σ_n^2 term. The noise bandwidth, and hence σ_n^2 is different in the cases of contiguous and non-contiguous bands because of the different observation bandwidth.

VI. Conclusion

We have rederived matrix formulae for linear models of static nonlinear MIMO systems, in which the distortion noise is uncorrelated to the input signals, and related them to the cumulant expansion of multivariate Gaussian processes distorted by static nonlinear functions. Formulae specific for nonlinear systems with a linear term are given. The formulae contain the input signals' covariance, the covariance of the input and output signals, and the covariance of the output signals. The most significant difference from the SISO Bussgang theorem is that the matrix formulation contains the covariance of the input signals. The case when one signal is a linear combination of other input signals results in a problem with lower rank and we have showed how to treat such a problem within the given framework. The importance of the correct observation bandwidth is emphasized as well as its effect on additive thermal noise.

We analyze the nonlinear distortion of concurrent dual and multiband transmitters for the cases of contiguous and non-contiguous bands. In such transmitters the signals are fed through the same nonlinear amplifier and Bussgang's theorem for SISO systems is not applicable.

For a concurrent dual band transmitter with non-contiguous bands, the cases of uncorrelated, correlated, and partly correlated input signals were analyzed. Correlated input signals give higher NMSE values for the same input power. For partly correlated signals, the matrices $\mathbf{A}$ and $\mathbf{V}$ are non-diagonal and the elements of $\mathbf{A}$ and $\mathbf{V}$ and the NMSE lie in between those for uncorrelated and correlated signals. A good understanding of the effects of nonlinear distortion on the NMSE can therefore be gained by analyzing the cases of correlated or uncorrelated signals, which is easier particularly for the case of concurrent non-contiguous multiband transmitters. For these the NSME is higher for correlated than for uncorrelated input signals and increase with the number of bands. The effect of finite number of sub-carriers in the OFDM signals is small compared to effect of the typical errors in the experimentally determined coefficients for the nonlinearities.

For transmitters with contiguous bands the aggregated output signal is analyzed. The matrix $\mathbf{A}$ contains a time dependent term which is an effect of different center frequencies.

The presented analysis of nonlinear multiband transmitters using the matrix form of Bussgang's theorem could find further applications in the analysis of system performance of wireless systems with such transmitters. It could also be used to analyze the effect of nonlinear distortion in multiband receivers and decoders for such receivers. The matrix formalism makes it suitable when analyzing the effects of nonlinearities in multiband transmitters in conjunction with other hardware impairments.

References

[1] J. J. Bussgang, "Cross-correlation function of amplitude-distorted Gaussian signals," Res. Lab. Elec., Massachusetts Inst. Technol., Cambridge, MA, USA, Tech. Rep. 216, Mar. 1952.

[2] E. Costa, M. Midrio, and S. Pupolin, "Impact of amplifier nonlinearities on OFDM transmission system performance," *IEEE Commun. Lett.*, vol. 3, no. 2, pp. 37–39, Feb. 1999.

[3] H.E. Rowe, "Memoryless nonlinearities with Gaussian inputs: Elementary results," *Bell Syst. Tech. J.*, vol. 61, no. 7, pp. 1519–1525, Sep. 1982.

[4] M. Enqvist and L. Ljung, "Linear approximations of nonlinear FIR systems for separable input processes," *Automatica*, vol. 41, pp. 459–473, 2005.

[5] M. Schoukens and K. Tiels, "Identification of block-oriented nonlinear systems starting from linear approximations: A survey," *Automatica*, vol. 85, pp. 272–292, 2017.

[6] G. Jacovitti, A. Neri, and R. Cusani, "Methods for estimating the autocorrelation function of complex Gaussian stationary processes," *IEEE Trans. Acoust., Speech, Signal Process.*, vol. ASSP-35, no. 8, pp. 1126–1138, Aug. 1987.

[7] H. Bouhadda, H. Shaiek, D. Roviras, R. Zayani, Y. Medjahdi, and R. Bouallegue, "Theoretical analysis of BER performance of nonlinearly amplified FBMC/OQAM and OFDM signals," *Eurasip J. Adv. Signal Process.*, vol. 2014, Feb. 2014, Art. no. 60.

[8] J. Guerreiro, D. Dinis, and P. Montezuma, "On the optimum multicarrier performance with memoryless nonlinearities," *IEEE Trans. Commun.*, vol. 63, no. 2, pp. 498–509, Feb. 2015.
[9] K. M. Gharaibeh, K. G. Gard, and M. B. Steer, "Estimation of co-channel nonlinear distortion and SNDR in wireless systems," *IET Microw. Antennas Propag.*, vol. 5, no. 5, pp. 1078–1085, 2007.
[10] P. Drotr, J. Gazda, P. Galajda, D. Kocur, and Pavelka,"Receiver technique for iterative estimation and cancellation of nonlinear distortion in MIMO SFBC-OFDM systems," *IEEE Trans. Consum. Electron.*, vol. 56, no. 2, pp. 471–475, May 2010.
[11] L. Cheded, "Invariance property of Gaussian signals: A new interpretation, extension and applications," *Circuits, Syst. Signal Process.*, vol. 16, no. 5, pp. 523–536, 1997.
[12] G. Scarano, "Cumulant series expansion of hybrid nonlinear moments of complex variables," *IEEE Trans. Signal Process.*, vol 39, no, 4, pp. 1001–1003, Apr. 1991.
[13] P. Händel and D. Rönnow, "Dirty MIMO transmitters: Does it matter?" *IEEE Trans. Wireless Commun.*, vol. 17, no. 8, pp. 5425–5436, Aug. 2018.
[14] M. C. Dahkli, R. Zayani, O. B. Belkacem, and R. Bouallegue, "Theoretical analysis and compensation for the joint effects of HPA nonlinearity and RF crosstalk in VBLAST MIMO-OFDM systems over Rayleigh fading channel," *EURASIP J. Wireless Commun. Netw.*, vol. 2014, Apr. 2014, Art. no. 61.
[15] T. P. Dobrowiecki and J. Schoukens, "Linear approximation of weakly nonlinear MIMO systems," *IEEE Trans. Instrum. Meas.*, vol. 56, no. 3, pp. 887–894, Jun. 2007.
[16] A. Mezghani and J. A. Nossek, "Capacity lower bound of MIMO channels with output quantization and correlated noise," in *Proc. IEEE Int. Symp. Inf. Theory*, Jul. 2012, pp. 1–5.
[17] S. Jacobsson, G. Durisi, M. Coldrey, T. Goldstein, and C. Studer, "Quantized precoding for massive MU-MIMO," *IEEE Trans. Commun.*, vol 65, no. 11, pp. 4670–4684, Nov. 2017.
[18] A. K. Saxena, I. Fijalkow, and A. L. Swindlehurst, "Analysis of one-bit quantized precoding for the multiuser massive MIMO downlink," *IEEE Trans. Signal Process.*, vol. 65, no. 17, pp. 4624–4634, Sep. 2017.
[19] O. De Candido, H. Jedda, A. Mezghani, A. L. Swindlehurst, and J. A. Nossek, "Reconsidering linear transmit signal processing in 1-bit quantized multi-user MISO systems," *IEEE Trans. Wireless Commun.*, vol. 18, no. 1, pp. 254–267, Jan. 2019.
[20] Q. Hou, R. Wang, E. Liu, and D. Yan, "Hybrid precoding design for MIMO system with one-bit ADC receivers," *IEEE Access*, vol. 6, pp. 48478–48488, 2018.
[21] Y. Li, C. Tao, G. S.-Granados, A. Mezghani, A. L. Swindlehurst, and L. Liu, "Channel estimation and performance analysis of one-bit massive MIMO systems," *IEEE Trans. Signal Process.*, vol. 65, no. 15, pp. 4075–4089, May 2017.
[22] E. Björnson, L. Sanguinetti, and J. Hoydis, "Hardware distortion correlation has negligible impact on UL massive MIMO spectral efficiency," *IEEE Trans. Commun.*, vol. 67, no. 2, pp. 1085–1098, Feb. 2019.
[23] F. Wendler, M. Stein, A. Mezghani, and J. A. Nossek, "Quantization-loss reduction for 1-bit BOC positioning," in *Proc. IEEE Int. Symp. Inf. Theory*, Jan. 2013, pp. 509–518.
[24] S. A. Bassam, W. Chen, M. Helaoui, and F. M. Ghannouchi, "Transmitter architecture for CA: Carrier aggregation in LTE-advanced systems," *IEEE Microw. Mag.*, vol. 14, no. 5, pp. 78–86, Jul. 2013.
[25] S. Kang, U. Kim, and J. Kim, "A multi-mode multi-band reconfigurable power amplifier for 2G/3G/4G handset applications," *IEEE Microw. Wireless Compon. Lett.*, vol. 25, no. 1, pp. 49–51, Jan. 2015.
[26] R. Han, W. Yang, and K. You, "MB-OFDM-UWB based wireless multimedia sensor networks for underground coalmine: A survey," *Sensors*, vol. 16, pp. 2158–2178, Dec. 2016
[27] M. Z. Farooqi, S. M. Tabassum, M. H. Rehmani, and Y. Saleem, "A survey on network coding: From traditional wireless networks to emerging cognitive radio networks," *J. Netw. Comp. Appl.*, vol. 46, pp. 166–181, Sep. 2014.
[28] G. Scarano, D. Caggiati, and G. Jacovitti, "Cumulant expansion of hybrid nonlinear moments of *n* variates," *IEEE Trans. Signal Process.*, vol. 41, vo. 1, pp. 486–489, Jan. 1993.
[29] P. J. Schreier and L. L. Scharf, *Statistical Signal Processing of Complex-Valued Data. The Theory of Improper and Noncircular Signals*. Cambridge, U.K.: Cambridge Univ. Press, 2010.
[30] R. M. Range, *Holomorphic Functions and Integral Representations in Several Complex Variables*. New York, NY, USA: Springer, 1998.
[31] P. O. Amblard, M. Gaeta, and J. L. Lacoume, "Statistics for complex variables and signals—Part I: Variables," *Signal Process.*, vol. 53, pp. 1–13, 1996.
[32] C. Mollén, "High-end performance with low-end hardware: Analysis of massive MIMO base station transceivers," PhD dissertation, Faculty Sci. Eng., Linköping Univ., Linköping, Sweden, 2017.
[33] D. Dardari, V. Tralli, and A. Vaccari, "A theoretical characterization of nonlinear distortion effects in OFDM systems," *IEEE Trans. Commun.*, vol. 48, no. 10, pp. 1755–1764, Feb. 2000.
[34] D. M. Pozar, *Microwave Engineering*, 4th ed. Hoboken, NJ, USA: Wiley, 2012.
[35] F. Ghannouchi, M. Younes, and R. Rawat, "Distortion and impairments mitigation and compensation of single- and multi-band wireless transmitters (invited)," *IET Microw. Antennas Propag.*, vol. 7, no. 7, pp. 518–534, 2013.
[36] S. Amin, W. Van Moer, P. Händel, and D. Rönnow, "Characterization of concurrent dual-band power amplifiers using a dual two-tone excitation signal," *IEEE Trans. Instrum. Meas.*, vol. 64, no. 10, pp. 2781–2791, Oct. 2015.
[37] P. Händel, "Understanding normalized mean squared error in power amplifier linearization," *IEEE Microw. Wireless Compon. Lett.*, vol. 28, no. 11, pp. 1047–1049, Nov. 2018.
[38] E. Rubiola and F. Vernotte, "The cross-spectrum experimental method," 2010, *arXiv:1003.0113*.
[39] F. Gustafsson, *Statistical Sensor Fusion*. Lund, Sweden: Studentlitteratur, 2012, pp. 22–28.
[40] T. Söderström and P. Stoica, *System Identification*, 2nd ed. Hemel Hempstead, U.K.: Prentice-Hall, 2001, ch. 4.
[41] T. Araujo, and R. Dinis, "On the accuracy of the Gaussian approximation for the evaluation of nonlinear effects in OFDM signals," *IEEE Trans. Commun.*, vol. 60, no. 2, pp. 346–351, Feb. 2012.
[42] Keysight Technologies, Inc., "LTE physical layer overview," [Online]. Available: rfmw.em.keysight.com/wireless/helpfiles/89600b/webhelp/subsystems/lte/content/lte_verview.htm. Accessed on: Apr. 17, 2019.

Daniel Rönnow (M'04) received the M.Sc. degree in engineering physics and the Ph.D. degree in solid state physics from Uppsala University, Uppsala, Sweden, in 1991 and 1996, respectively. He was with the Max Planck Institute, Stuttgart, Germany, from 1996 to 1998, and with Acreo AB, Stockholm, Sweden, from 1998 to 2000. From 2000 to 2004, he was with Racomna AB, Uppsala, Sweden. From 2004 to 2006, he was a University Lecturer with the University of Gvle, Gvle, Sweden, where he became a Professor of Electronics in 2011. From 2006 to 2011, he was a Senior Sensor Engineer with WesternGeco, Oslo, Norway. He has been an Associate Professor with Uppsala University since 2000. He has authored or co-authored more than 60 peer-reviewed journal papers. He holds eight patents. His current research interests are RF measurement techniques and linearization of nonlinear RF circuits and systems.

Peter Händel (S'88–M'94–SM'98) received the M.Sc. degree in engineering physics and the Lic.Eng. and Ph.D. degrees in automatic control from the Department of Technology, Uppsala University, Uppsala, Sweden, in 1987, 1991, and 1993, respectively. He held a part-time position as an Associate Director of Research with the Swedish Defense Research Agency from 2000 to 2006. In 2010, he joined the Indian Institute of Science, Bangalore, India, as a Guest Professor. He was a Guest Professor with the University of Gvle between 2007 and 2013. Since 1997, he has been with the Royal Institute of Technology (KTH), Stockholm, Sweden, where he is currently a Professor of Signal Processing with the School of Electrical Engineering and Computer Science. He has authored more than 300 scientific publications. He was a recipient of a number of awards, including the IEEE TRANSACTIONS ON INTELLIGENT TRANSPORTATION SYSTEMS Best Survey Paper Award. He is the former President of the IEEE Finland Joint Signal Processing and Circuits and Systems Chapter and the former President of the IEEE Sweden Signal Processing Chapter. He was an Associate Editor for the IEEE TRANSACTIONS ON SIGNAL PROCESSING.